

Cite this: *Chem. Commun.*, 2011, **47**, 1985–1987

www.rsc.org/chemcomm

## COMMUNICATION

## Photo-induced magnetic bistability in a controlled assembly of anisotropic coordination nanoparticles†

Florence Volatron,<sup>a</sup> Daniela Heurtaux,<sup>a</sup> Laure Catala,<sup>\*a</sup> Corine Mathonière,<sup>\*b</sup> Alexandre Gloter,<sup>c</sup> Odile Stéphan,<sup>c</sup> Diego Repetto,<sup>b</sup> Miguel Clemente-León,<sup>\*d</sup> Eugenio Coronado<sup>d</sup> and Talal Mallah<sup>a</sup>

Received 12th November 2010, Accepted 22nd December 2010

DOI: 10.1039/c0cc04940a

Anisotropic coordination nanoparticles of the photomagnetic network  $\text{Cs}_2\text{Cu}^{\text{II}}_7[\text{Mo}^{\text{IV}}(\text{CN})_8]_4$  are obtained through a surfactant-free high-yield synthetic procedure in water. These particles are organised as Langmuir–Blodgett films with a preferential orientation of the nano-objects within the film that exhibit a magnetic bistability below 20 K with a very large coercivity due to an efficient photo-transformation.

Photomagnetic cyanide-based coordination networks are appealing systems since their magnetic behavior can be tuned by light.<sup>1,2</sup> One important challenge is to design nano-objects that display a photo-induced *magnetic* bistability, with the aperture of a hysteresis loop in the photo-induced ferromagnetic state. A few examples of photomagnetic molecules have been reported and their photomagnetic studies evidenced that a reversible photo-switching may be preserved at the level of a few metallic centers.<sup>3</sup> However, none of these systems shows a photo-induced magnetic bistability. Coordination nanoparticles (CNPs) of photomagnetic networks<sup>4,5</sup> that possess a larger number of metallic centres than molecules may be excellent candidates to exhibit a ferromagnetic ordering or a blocking of their magnetisation after irradiation; to date this has clearly been demonstrated on nanoparticles of a few nanometres in one case.<sup>6</sup> To favor such a magnetic bistability, a main requirement is to photo-transform efficiently the sample. Up to now, photomagnetic films of nano-objects displaying a magnetic bistability have never been reported.

The Langmuir–Blodgett (LB) technique, that has been applied to a few magnetic and electrochromic CNPs,<sup>7</sup> is among the best methods to reach this goal. A main condition for the implementation of this technique is to have dispersable particles. We have previously shown that water-soluble CNPs based on hexacyanometalates can be synthesized.<sup>8,9</sup> In this communication, we demonstrate that the same approach can be extended to the objects based on the potentially photo active complex  $\text{Mo}(\text{CN})_8^{4-}$ . We report here a straightforward synthesis in water of charged anisotropic particles of the cyanide-bridged network  $\text{Cs}_2\text{Cu}^{\text{II}}_7[\text{Mo}^{\text{IV}}(\text{CN})_8]_4$  that allows their easy processing in different matrices and as multilayer films. All the samples reveal a photo-induced magnetic bistability, and the LB film displays a photo-induced large coercive field as a result of a remarkable enhancement of the photo-transformation.

The photomagnetic octacyanometalate-based network  $\text{Cs}_2\text{Cu}^{\text{II}}_7[\text{Mo}^{\text{IV}}(\text{CN})_8]_4$  was initially reported by Hozumi *et al.* as single crystals and films prepared by electrochemical synthesis through the reduction of  $\text{Mo}^{\text{V}}(\text{CN})_8^{3-}$ .<sup>2</sup> In our procedure, charged nanoparticles are prepared directly starting from  $\text{Mo}^{\text{IV}}(\text{CN})_8^{4-}$  by a facile, large scale and high yield method, based on the fast introduction of the precursors in water while keeping an excess of octacyanometalate with respect to the copper salt.† Dynamic Light Scattering (DLS) and  $\zeta$ -potential give a hydrodynamic diameter of 15 nm and a value of  $-30$  mV, respectively, which are constant for several weeks (Fig. S1, ESI†). This evidences the negative charge responsible for the high stability of the particles over time. The purple color of the solution originates from the presence of the intervalence band  $\text{Mo}(\text{IV})\text{Cu}(\text{II})\text{--}\text{Mo}(\text{V})\text{Cu}(\text{I})$  at 515 nm (Fig. S2, ESI†) similarly to that of the reference compound.<sup>2</sup>

Such charged nanoparticles were post-functionalised by a cationic surfactant dioctadecyl dimethyl ammonium ( $\text{CsCuMo\_DODA}$  sample) or polyvinylpyrrolidone ( $\text{CsCuMo\_PVP}$  sample) to obtain isolated particles in different environments.<sup>5,8,10</sup> The solid-state IR spectrum on the  $\text{CsCuMo\_DODA}$  revealed peaks at  $2158\text{ cm}^{-1}$  and  $2105\text{ cm}^{-1}$  that are assigned to the asymmetric vibration of the  $\text{Mo}(\text{IV})\text{--}\text{CN--}\text{Cu}(\text{II})$  entities and the non-bridging octacyanomolybdates located at the surface of the particles respectively. Transmission Electronic Microscopy (TEM) performed on

<sup>a</sup> Institut de Chimie Moléculaire et des Matériaux d'Orsay, CNRS, Université Paris 11, 91405 Orsay, France.

E-mail: laure.catala@u-psud.fr; Fax: +33169154754; Tel: +33169157890

<sup>b</sup> CNRS, Université de Bordeaux, ICMCB, 87 avenue du Dr. Albert Schweitzer, Pessac, F-33608, France. E-mail: mathon@icmcb-bordeaux.cnrs.fr

<sup>c</sup> Laboratoire de Physique des Solides, UMR 8502, Université Paris-Sud 11, F-91405 Orsay, France

<sup>d</sup> Instituto de Ciencia Molecular, Universitat de Valencia, Catedrático José Beltrán 2, 46980 Paterna, Spain. E-mail: miguel.clemente@uv.es

† Electronic supplementary information (ESI) available: Elemental analysis, structure, experimental procedures, dynamic light scattering, UV-vis and IR spectra, X-Ray Powder diagrams, AFM and TEM images, additional photomagnetic measurements, thickness profiles. See DOI: 10.1039/c0cc04940a

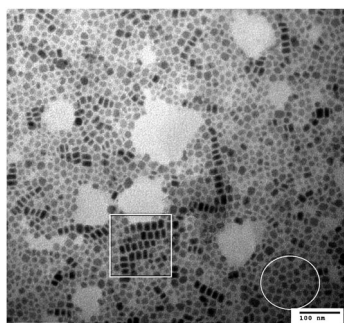


**Fig. 1** TEM image of the CsMoCu\_DODA nanoparticles (inside square: perpendicular orientation, inside circle: parallel orientation), scale bar = 100 nm.

CsMoCu\_DODA dispersed in chloroform shows nanoparticles well separated due to the interpenetrated chains of DODA<sup>+</sup> (Fig. 1). The nanoparticles have an anisotropic platelet-like morphology, and are observed either with their larger face parallel (hexagon-like particles) or perpendicular to the grid (giving a rod-like projection, see also Fig. S3, ESI†). The statistics performed on 200 particles revealed a size of 16.3 nm ( $\sigma = 2.9$  nm) for the larger face and a thickness of 9.5 nm ( $\sigma = 2.0$  nm) with a length/width ratio of 1.7 (Fig. S3, ESI†). Electron Energy Loss Spectroscopy performed in the High Angular Dark Field mode obtained by Scanning TEM attests that all the particles contain Cs and Cu (Fig. S4, ESI†). Importantly, X-ray powder diffraction confirmed that the tetragonal bilayered structure of the Cs<sub>1.2</sub>Cu<sub>1.7</sub>[Mo<sup>IV</sup>(CN)<sub>8</sub>]<sub>4</sub> network is retained for the nanoparticles (Fig. S5, ESI†).<sup>2</sup> Comparison of the elemental analysis of the two samples (see ESI†) allows us to determine the exact composition of the inorganic core [Cs<sub>0.5</sub>Cu<sup>II</sup><sub>1.75</sub>[Mo<sup>IV</sup>(CN)<sub>8</sub>]<sub>1.1</sub>]<sup>0.4-</sup> that evidences the negative charge born by the particles due to the incorporation of a slight excess of [Mo<sup>IV</sup>(CN)<sub>8</sub>]<sup>4-</sup>.

Thanks to the stability of the particles in water, they may be easily processed as multilayer LB films on various substrates (Fig. S6, ESI†) with a DODABr Langmuir monolayer spread at the water-interface as reported for other CNPs.<sup>11</sup> IR spectrum of the film is similar to that of the CsMoCu\_DODA sample (Fig. S7, ESI†). Atomic Force Microscopy (AFM) on one monolayer transferred on a glass support shows a rather homogeneous film height of about 10 nm, corresponding to the thickness of the particles with some rare spots (less than 10%) about 15 nm high (Fig. 2 and Fig. S8 (ESI†)). TEM observation of one monolayer deposited on a grid shows only the larger facets of the particles with a size distribution in agreement with that of the CsMoCu\_DODA sample

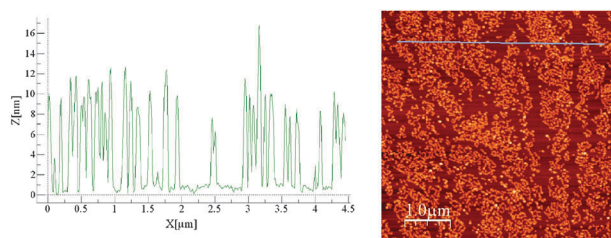


**Fig. 2** AFM image and height profile on a LB film of one layer of nanoparticles deposited on a glass substrate.

(Fig. S9, ESI†). Hence, orientation of the larger facets of the CNPs parallel to the substrate forming the monolayer is demonstrated by both AFM and TEM measurements, and this orientation is maintained in the multilayer film (Fig. S10, ESI†).

The photomagnetic studies were performed on the samples CsMoCu\_DODA and CsMoCu\_PVP containing randomly oriented particles (see ESI†). The  $\chi T = f(T)$  plots (Fig. S11, ESI†) after blue light irradiation reveal for both samples the appearance of ferromagnetic interactions that may be due either to a photo-induced electron transfer from the diamagnetic Mo<sup>IV</sup> to the Cu<sup>II</sup> centres that generate ferromagnetic interactions between the Mo<sup>V</sup> and the remaining Cu<sup>II</sup> sites or to the recently proposed mechanism involving a photo-induced high spin Mo<sup>IV</sup> species.<sup>12</sup> Magnetization *vs.* field studies performed on CsMoCu\_DODA and CsMoCu\_PVP show an increase of the magnetization after irradiation with a maximum value at 5 T and 5 K of 1.15 and 1.20  $\mu_B$  respectively (Fig. S11, ESI†). The two systems turn to the initial state upon heating above 200 K. Similar  $\chi T$  and magnetization values for both samples indicate that the photo-transformation is mainly the same in the two samples (Fig. S11 and S12, ESI†). Magnetization *vs.* temperature studies were carried out on both samples after irradiation and reveal a sharp increase below 15 K and 10 K respectively (Fig. S13, ESI†). The hysteresis loops measured at 2 K after irradiation show coercive fields of 367 and 67 Oe for CsMoCu\_DODA and CsMoCu\_PVP respectively (Fig. S14, ESI†). The difference between the two samples observed on the  $M = f(T)$  curves and coercive fields may be attributed to the weaker dipolar interactions between the nanoparticles in the case of the PVP sample.

In order to obtain a detectable photomagnetic response, a film 200 nm thick of oriented CNPs was deposited (45 deposition cycles) on a mylar substrate (Fig. S14, ESI†) and studied in similar conditions. The magnetization monitored *vs.* time at 10 K ( $H = 100$  Oe) shows a dramatic increase during the irradiation process (Fig. 3a). After irradiation, the zero-field cooled and field-cooled magnetizations display a

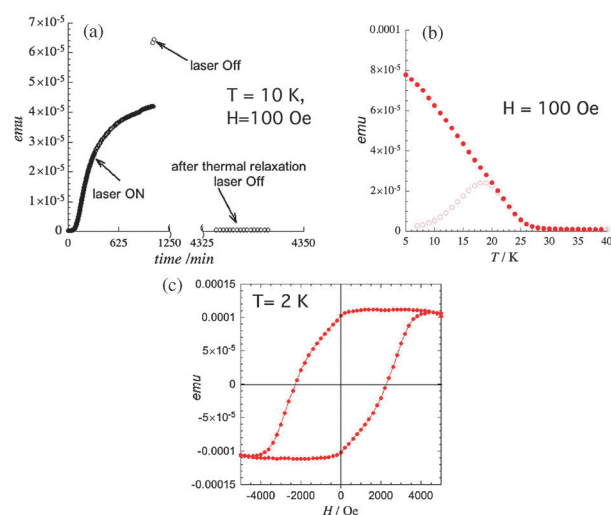


**Fig. 3** (a) Kinetic evolution of the magnetization at 10 K during irradiation and after thermal treatment at 200 K, (b) field-cooled and zero-field cooled magnetizations (sweeping rate 0.4 K min<sup>-1</sup>) and (c)  $M = f(H)$  measured at  $T = 2$  K; all measurements are obtained on the LB film.

divergence below 23 K (Fig. 3b) at temperatures close to that reported on the electrocrystallised film.<sup>2</sup>

Moreover, the hysteresis loop measured at 2 K reveals a remarkably large coercive field of 2300 Oe (Fig. 3c), six times larger than the reference compound ( $H_C = 350$  Oe).<sup>2</sup> The recovery of the initial magnetization value was obtained after thermal treatment at 200 K (Fig. 3a). This photo-induced hysteresis loop was reproduced on three LB films made with different batches of particles.

The light-induced magnetic bistability of the CsMoCu nanoparticles occurs in the randomly oriented particles within the DODA and the PVP matrices. While, the oriented assembly of the anisotropic CNPs in the LB film leads to a remarkable coercivity enhancement (above 2300 Oe) compared to the randomly oriented particles or to the electrocrystallized films. One hypothesis to explain the large coercive field of the LB film is the presence of stronger dipolar interactions (due to a larger magnetic moment combined to short interparticle distances) between the fully photo-converted objects that are promoted by a better photo-transformation within the LB film than in the PVP and the DODA matrices. This is supported by the fact that the increase of the magnetization before and after irradiation reaches a ratio of nearly 300 on the LB film, while a ratio of 68 is obtained on the CsMoCu\_DODA without achieving saturation (Fig. 3a and Fig. S16 (ESI†)).

This communication highlights two important issues: (i) the spontaneous stabilization of anisotropic nanoobjects in water without the presence of coating agents and (ii) their oriented assembly as transparent films that allowed an enhanced photo-transformation and thus the occurrence of light-induced magnetic bistability below 23 K with a large coercive field.

We thank the CNRS, the French programme ANR-blanc (project MS-MCNP n° BLAN07-2\_191699), the Spanish Ministerio de Ciencia e Innovación, with FEDER cofinancing (Projects Consolider-Ingenio in Molecular Nanoscience, MAT2007-61584, and CTQ2008-06720), the Generalitat Valenciana (Project PROMETEO/2008/128) and the European community (MolSpinQIP, SPINMOL ERC Advanced Grant) for financial support. We thank Ángel López-Muñoz for the preparation and characterization (IR, TEM and thickness determination) of the LB films.

## Notes and references

† In a 1 L Erlenmeyer, 300 mL of an aqueous solution of CsCl (4 mM) and CuSO<sub>4</sub> (2 mM) were added under vigorous stirring (800 t min<sup>-1</sup>) on a 300 mL aqueous solution of K<sub>4</sub>Mo(CN)<sub>8</sub> (2 mM). An immediate change of colour to purple occurred. The CsMoCu\_DODA sample is obtained by adding dropwise 300 mL of the aqueous solution to 600 mL of a 6 mM methanolic solution of DODABr under vigorous stirring. A purple precipitate appeared that was centrifuged at 10 000 t min<sup>-1</sup> during 15 min and dried under vacuum. The CsMoCu\_PVP sample is obtained by adding 2.22 g of PVP to 200 mL of the aqueous solution. 600 mL of acetone were added in the solution and the precipitate was centrifuged at 10 000 t min<sup>-1</sup> during 15 min and dried under vacuum. § These characterizations were performed on three different films prepared from different batches of CNPs and revealed similar features.

- Z. Z. Gu, O. Sato, T. Iyoda, K. Hashimoto and A. Fujishima, *J. Phys. Chem.*, 1996, **100**, 18289–18291; O. Sato, T. Iyoda, A. Fujishima and K. Hashimoto, *Science*, 1996, **272**, 704–705; A. Bleuzen, C. Lomenech, V. Escax, F. Villain, F. Varret, C. C. D. Moulin and M. Verdaguer, *J. Am. Chem. Soc.*, 2000, **122**, 6648–6652; G. Champion, V. Escax, C. C. D. Moulin, A. Bleuzen, F. O. Villain, F. Baudet, E. Dartyge and N. Verdaguer, *J. Am. Chem. Soc.*, 2001, **123**, 12544–12546; Y. Arimoto, S.-i. Ohkoshi, Z. J. Zhong, H. Seino, Y. Mizobe and K. Hashimoto, *J. Am. Chem. Soc.*, 2003, **125**, 9240–9241; S.-i. Ohkoshi, S. Ikeda, T. Hozumi, T. Kashiwagi and K. Hashimoto, *J. Am. Chem. Soc.*, 2006, **128**, 5320–5321; S.-i. Ohkoshi, H. Tokoro, T. Hozumi, Y. Zhang, K. Hashimoto, C. Mathonière, I. Bord, G. Rombaut, M. Verelst, C. C. D. Moulin and F. Villain, *J. Am. Chem. Soc.*, 2006, **128**, 270–277; O. Sato, J. Tao and Y. Z. Zhang, *Angew. Chem., Int. Ed.*, 2007, **46**, 5049; H. Tokoro, T. Matsuda, T. Nuida, Y. Moritomo, K. Ohoyama, E. D. L. Dangui, K. Boukheddaden and S.-i. Ohkoshi, *Chem. Mater.*, 2008, **20**, 423–428; D. M. Pajerowski, J. E. Gardner, D. R. Talham and M. W. Meisel, *J. Am. Chem. Soc.*, 2009, **131**, 12927–12936; D. M. Pajerowski, M. J. Andrus, J. E. Gardner, E. S. Knowles, M. W. Meisel and D. R. Talham, *J. Am. Chem. Soc.*, 2010, **132**, 4058–4059.
- T. Hozumi, K. Hashimoto and S.-i. Ohkoshi, *J. Am. Chem. Soc.*, 2005, **127**, 3864–3869.
- J. M. Herrera, V. Marvaud, M. Verdaguer, J. Marrot, M. Kalisz and C. Mathonière, *Angew. Chem., Int. Ed.*, 2004, **43**, 5468–5471; J. Long, L. M. Chamoiseau, C. Mathonière and V. Marvaud, *Inorg. Chem.*, 2009, **48**, 22–24; D. F. Li, R. Clérac, O. Roubeau, E. Harte, C. Mathonière, R. Le Bris and S. M. Holmes, *J. Am. Chem. Soc.*, 2008, **130**, 252–258.
- J. G. Moore, E. J. Lochner, C. Ramsey, N. S. Dalal and A. E. Stiegman, *Angew. Chem., Int. Ed.*, 2003, **42**, 2741–2743; F. A. Frye, D. M. Pajerowski, J. H. Park, M. W. Meisel and D. R. Talham, *Chem. Mater.*, 2008, **20**, 5706–5713; G. Fornasieri and A. Bleuzen, *Angew. Chem., Int. Ed.*, 2008, **47**, 7750–7752; D. M. Pajerowski, F. A. Frye, D. R. Talham and M. W. Meisel, *New J. Phys.*, 2007, **9**, 222; G. Fornasieri, M. Aouadi, P. Durand, P. Beaunier, E. Rivière and A. Bleuzen, *Chem. Commun.*, 2010, **46**, 8061–8063.
- L. Catala, C. Mathonière, A. Gloter, O. Stéphan, T. Gacoin, J. P. Boilot and T. Mallah, *Chem. Commun.*, 2005, 746–748.
- D. Brinzei, L. Catala, C. Mathonière, W. Wernsdorfer, A. Gloter, O. Stéphan and T. Mallah, *J. Am. Chem. Soc.*, 2007, **129**, 3778–3779.
- C. Mingotaud, C. Lafuente, J. Amiel and P. Delhaes, *Langmuir*, 1999, **15**, 289–292; G. R. Torres, E. Dupart, C. Mingotaud and S. Ravaine, *J. Phys. Chem. B*, 2000, **104**, 9487–9490; S. Bharathi, M. Nogami and S. Ikeda, *Langmuir*, 2001, **17**, 7468–7471; G. R. Torres, A. Agricole, P. Delhaes and C. Mingotaud, *Chem. Mater.*, 2002, **14**, 4012–4014; G. Romualdo-Torres, B. Agricole, C. Mingotaud, S. Ravaine and P. Delhaes, *Langmuir*, 2003, **19**, 4688–4693.
- D. Brinzei, L. Catala, N. Louvain, G. Rogez, O. Stéphan, A. Gloter and T. Mallah, *J. Mater. Chem.*, 2006, **16**, 2593–2599.
- L. Catala, D. Brinzei, Y. Prado, A. Gloter, O. Stéphan, G. Rogez and T. Mallah, *Angew. Chem., Int. Ed.*, 2009, **48**, 183–187.
- L. Catala, T. Gacoin, J. P. Boilot, E. Rivière, C. Paulsen, E. Lhotel and T. Mallah, *Adv. Mater.*, 2003, **15**, 826–829; L. Catala, A. Gloter, O. Stéphan, G. Rogez and T. Mallah, *Chem. Commun.*, 2006, 1018–1020.
- M. Clemente-Leon, E. Coronado, A. Lopez-Munoz, D. Repetto, C. Mingotaud, D. Brinzei, L. Catala and T. Mallah, *Chem. Mater.*, 2008, **20**, 4642–4652.
- M. A. Arrio, J. Long, C. C. D. Moulin, A. Bachschmidt, V. Marvaud, A. Rogalev, C. Mathonière, F. Wilhelm and P. Saintavrit, *J. Phys. Chem. C*, 2010, **114**, 593–600.